PHOTON CORRELATION SPECTROSCOPY OF BILAYER LIPID MEMBRANES

J. F. CRILLY AND J. C. EARNSHAW
Department of Pure and Applied Physics, The Queen's University of Belfast, Belfast, Northern Ireland

ABSTRACT Light scattering by thermal fluctuations on simple monoglyceride bilayer membranes has been used to investigate the viscoelastic properties of these structures. Spectroscopic analysis of these fluctuations (capillary waves) permits the nonperturbative measurement of the interfacial tension and a shear interfacial viscosity acting normal to the membrane plane. The methods were established by studies of solvent and nonsolvent bilayers of glycerol monooleate (GMO). Changes in the tension of GMO/*n*-decane membranes induced by altering the composition of the parent solution were detected and quantified. In a test of the reliability of the technique controlled variations of the viscosity of the aqueous bathing solution were accurately monitored. The technique was applied to solvent-free bilayers formed from dispersions of GMO in squalane. The lower tensions observed attested to the comparative absence of solvent in such bilayers. In contrast to the solvent case, the solvent-free membranes exhibited a significant transverse shear viscosity, indicative of the enhanced intermolecular interactions within the bilayer.

INTRODUCTION

Biological membranes are ultrathin structures, only a few molecules thick, forming the interface between two fluid phases. These systems possess viscoelastic properties that relate to the molecular organization and interactions within the membrane. Real biomembranes are complex structures and the study of macroscopic properties of membranes can be most usefully approached via model systems. This paper reports the application of laser-light scattering to the measurement of such properties for black lipid membranes (BLM) in aqueous media. Grabowski and Cowen (1) have previously demonstrated the possibility of such measurements. Light scattering has the advantage that it does not perturb thermal equilibrium and can potentially be used to measure several macroscopic properties of the system simultaneously. Some preliminary aspects of the present work have been reported elsewhere (2, 3).

A fluid interface is not static but is continually subject to disturbances driven by thermal motions of the system. The interfacial agitation may be Fourier decomposed into a set of spatial modes of wave vector $\mathbf{q}$ ($= 2\pi/\Lambda$), which evolve with time subject to the viscoelastic properties of the interface and of the adjoining fluids. When q is sufficiently great these interfacial modes are usually known as capillary waves, being driven by forces of capillarity rather than gravity. A given mode propagates on the interface with a frequency that is mainly determined by the interfacial tension, and is damped at a rate governed by the viscous forces in the system. In general, as well as the viscosities of the adjoining fluids, there may be up to four distinguishable interfacial viscosities (4). They are identified as shear and dilational viscosities acting within and normal to the interface plane. One of these, dilation normal to the interface, plays no role in the propagation of capillary waves. According to hydrodynamic theory, for the case of a symmetric membrane (defined as one having the same fluid on either side) only the transverse shear viscosity is experimentally accessible to light scattering.

Interfacial capillary waves scatter light, acting as weak dynamic diffraction gratings that phase modulate the incident laser light. The power spectrum of the hydrodynamic fluctuations is exactly reproduced in the spectrum of the scattered light. The frequency shifts of the scattered light are small (measured in kilohertz) and can only be measured by optical heterodyn spectroscopy. In the present work the spectra were analyzed in the time domain using photon correlation. Such methods have been applied to free surfaces of liquids (5) and to monomolecular layers of amphiphilic molecules on an aqueous subphase (6). For symmetric membranes only two interface properties (tension and transverse shear viscosity) are accessible by light scattering, and unique values of these properties can be extracted from the observed correlation functions.

BLM formed from solutions of lipid in hydrocarbon solvents (e.g., decane) incorporate substantial fractions of solvent within their final structure. Consequently their properties will not be those of a true lipid bilayer. The presence of a solvent medium reduces the interactions of the acyl chains of the lipid molecules, leading to differences in the mechanical properties of solvent and nonsolvent membranes (7). In particular, the membrane fluidity, which reflects the freedom of motion of the acyl chains, is almost certainly reduced by the removal of solvent from the membrane interior.

The light scattering technique has been applied to solvent and nonsolvent bilayer membranes of glycerol monooleate. The differing viscoelastic properties in the two cases are reported here.

THEORETICAL BACKGROUND

The theoretical description of capillary waves on fluid interfaces is well established. In particular, Kramer (8) treats thermally excited waves that are on a thin membrane immersed in fluid. In general, shear, compression, and transverse modes may occur. Light is not scattered by the shear modes, and for a membrane isotropic within its plane, the shear modes decouple from the others. For a symmetric membrane the compression and transverse modes also decouple. These modes both scatter light, but the scattered intensities are very different (9). As a result of the characteristically small tension and large compressibility of BLM, the mean square amplitude of the transverse fluctuations is considerably larger than that of the compression modes. The intensity of light scattered by capillary waves is several orders of magnitude above that of longitudinal waves. In the present work only the transverse modes were observed.

A bilayer has two interfaces with the adjoining aqueous media. Generally, the film tension (γ_f) is inferred from measurement of the interfacial tension (γ) of the bulk lipid solution-water system, using $\gamma_f \simeq 2\gamma$ (where the contact angle is assumed very small). The two interfaces are coupled together; this coupling is incorporated in the theoretical treatment of bilayer mechanics. Light scattering directly yields values of mechanical properties that relate to the individual interfaces (e.g., γ).

Viscous dissipation within the membrane can be introduced into the hydrodynamic theory of capillary motion by permitting the elastic constants of the membrane to become positive definite response functions (10), expanding the tension to first order in ω as

$$\gamma = \gamma_0 - i\,\omega\,\gamma' \qquad (1)$$

where γ_0 is the static membrane tension and the term γ' is identified as a shear interfacial viscosity acting normal to the membrane. Other viscoelastic properties of the interface do not affect the propagation of tranverse capillary waves on a symmetric membrane.

Kramer's theory of capillary waves is only valid for wavelengths that are large compared with the membrane thickness, but small compared with its diameter. Within these limits both gravitation and the effects of the Plateau-Gibbs border can be ignored. Capillary modes can be represented by a one-dimensional plane wave:

$$\zeta(x,t) = \zeta_0 \exp\left[-i\,(qx + \omega t)\right]$$

where q is the real wave vector of the disturbance and ω is the complex temporal frequency:

$$\omega = \omega_0 - i\,\Gamma,$$

ω_0 being the wave frequency and Γ its damping coefficient.

The dispersion equation derived by Kramer (8) for a capillary wave on a thin symmetric membrane can be parameterized in the form

$$(S^2 + \tau' S + Y)\,(1 + 2S)^{1/2} - (\tau' S + Y) = 0, \qquad (2)$$

in terms of the reduced quantities

$$\tau = \frac{\rho}{2\eta q^2}\quad S = -i\omega\tau\quad Y = \frac{\gamma_0 \rho}{8\eta^2 q}\quad \tau' = \frac{\gamma' q}{4\eta}$$

where η and ρ are the viscosity and the density of the aqueous phase. Here, and subsequently, all square roots are taken to be those with positive real parts. Eq. 2 can be manipulated into the form of a complex polynomial of fourth degree that can be solved numerically. The roots of this polynomial correspond to either propagating or overdamped capillary modes depending upon the exact value of the parameter Y, the transition occurring at a certain critical value (in the limit $\gamma' = 0$, $Y_{crit} = 0.155$). Above Y_{crit} the dispersion equation has complex conjugate roots corresponding to damped oscillatory motion. Below Y_{crit} the equation yields two distinct real roots corresponding to nonpropagating modes. The behavior of S depends upon an interplay between the driving force of surface tension and the damping effect of γ'. Fig. 1 shows the effects of γ' upon S; they are greater for membranes of low tension. Y_{crit} increases in the presence of γ'. For low membrane tension overdamping occurs at experimentally accessible values of q (<2,000 cm^{-1}) even for low values of γ'(Fig. 2).

Analytic approximations for ω_0 and Γ are useful for relating these parameters to the physical properties of the system. For the simplest case, the limit where $\gamma' = 0$, initial analytic approximations to the roots of Eq. 2 (assuming $S << 1$) are, for $Y > Y_{crit}$,

$$\omega = \left(\frac{\gamma q^3}{2\rho}\right)^{1/2} - i\,\frac{\eta q^2}{\rho}.$$

and for $Y < Y_{crit}$

$$\Gamma_1 = \frac{\gamma q}{4\eta} \text{ and } \Gamma_2 = \frac{2\eta}{\rho} q^2.$$

As Y increases towards Y_{crit}, these overdamped modes merge into a single nonpropagating mode (Fig. 1).

Improved approximations to the roots of Eq. 2 can be found in the same limit. By factorizing the fourth-order polynomial into two terms quadratic in S with the constraint that any remainder terms should vanish

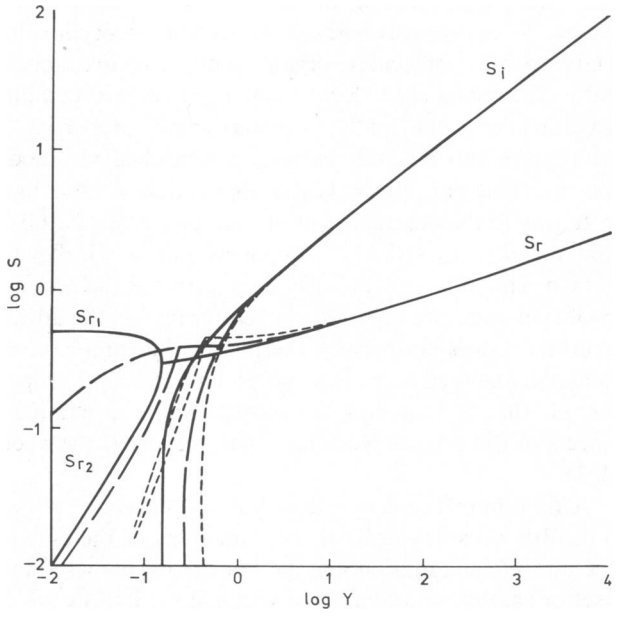

FIGURE 1 The roots of the dispersion equation (Eq. 2). S_r and S_i are the real and imaginary parts of the complex reduced frequency S. For BLM having typical values of tension, the physically realistic range of Y lies below 10. Below the critical value of Y the real roots are indicated by S_{r_1} and S_{r_2} Three different cases are shown: $\gamma' = 0$ (—) and $\gamma' = 1 \times 10^{-5}$ sP (surface poise or dyn s/cm) for tensions of 1 dyn/cm (---) and of 5 dyn/cm (— —). Note that the effect of a nonnegligible γ' is to decrease ω_0 and increase Γ above Y_{crit} and to reduce the difference between Γ_1 and Γ_2 below Y_{crit}. Both effects are more pronounced for low membrane tensions.

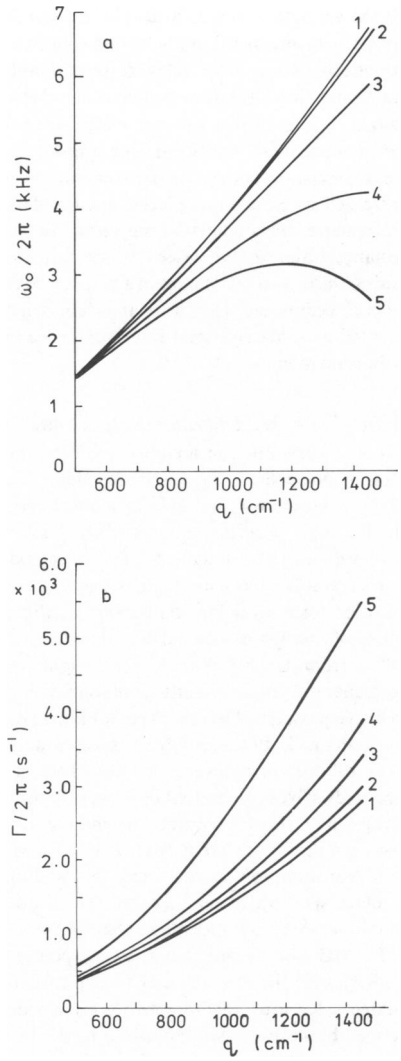

FIGURE 2 The frequencies ($\omega_0/2\pi$) and line widths ($\Gamma/2\pi$) of capillary waves on membranes of $\gamma_0 = 2$ dyn/cm where $\eta = 1$ cP. The numbered lines correspond to γ' values of 0 (1), 3.5×10^{-7} (*2*), 1.5×10^{-5} (*3*), 3.5×10^{-5} (*4*) and 5.0×10^{-5} sP (*5*). The trends of Fig. 1 are clearly evident.

(see Appendix) analytic expressions can be derived for $Y > Y_{crit}$:

$$\omega = \left(\frac{\gamma q^3}{2.3\rho}\right)^{1/2}\left(1 - \frac{1.2\eta^2 q}{\rho\gamma}\right)^{1/2} - i\left(\frac{0.85\eta q^2}{\rho} + \frac{0.03\gamma q}{8\eta}\right), \quad (3)$$

and for $Y < Y_{crit}$

$$\Gamma_1 = \frac{1.2\gamma q}{4\eta\,(1+\alpha)} \text{ and } \Gamma_2 = \frac{\eta q^2}{\rho}(1+\alpha), \quad (4)$$

where $\alpha = 1/2Y^{1/2}$.

This approach can be extended to the general case of nonnegligible γ'. The complex frequency derived (for $Y > Y_{crit}$) is

$$\omega = \left(\frac{\gamma_0}{2.3\rho}\right)^{1/2} q^{3/2}\left[1 - 1.5\,(1+\tau')^2\frac{\eta^2 q}{\gamma_0\rho}\right]^{1/2} - i\left[0.85\,(1+\tau')\frac{\eta}{\rho}q^2 + 0.03\frac{\gamma_0 q}{8\eta}\right]. \quad (5)$$

This reproduces the correct analytic dependence of ω_0 and Γ on both tension and transverse viscosity (Fig. 1). The increase in Y_{crit} is also correctly predicted by Eq. 5. In the high damping regime for which $Y < Y_{crit}$, S is small and Eq. 3 can be reduced to the form (11) $S^2 + (1+\tau')S + Y = 0$, which yields two real roots representing modes for which the observed correlation functions are a sum of exponentials having damping constants

$$\Gamma_1 \simeq -\left(\frac{\eta}{\rho}q^2\right)(1+\tau')\left[1 - \frac{\gamma_0\rho}{8\eta^2 q}(1-\tau')\right]$$

$$\Gamma_2 \simeq -\frac{\gamma_0 q}{4\eta}(1-\tau'). \quad (6)$$

All of the above approximations are only strictly valid within their regime of derivation. Where γ' is nonzero the assumption $\tau' \leq 0.5$ is most likely to restrict the validity of the derived formulae.

The spectrum of light scattered by the waves reflects their temporal evolution (8). Using the fluctuation-dissipation theorem in the classical limit the spectrum can be related to the complex admittance function of the system (for example, see reference 11). In the present case it can be shown that

$$P_q(\omega) = \frac{\tau^2 q}{2\rho}\frac{k_B T}{\pi\omega}\,Im\left[\frac{(1+2S)^{1/2} - 1}{(S^2 + \tau' S + Y)(1+2S)^{1/2} - (Y + \tau' S)}\right] \quad (7)$$

where k_B is the Boltzmann constant, T the temperature and Im (...) signifies the imaginary part of the function. The spectrum comprises a Brillouin doublet for $Y > Y_{crit}$ or two modes centered on $\omega = 0$ for $Y < Y_{crit}$. Far from Y_{crit} the spectrum is approximately Lorentzian (see Fig. 3), but

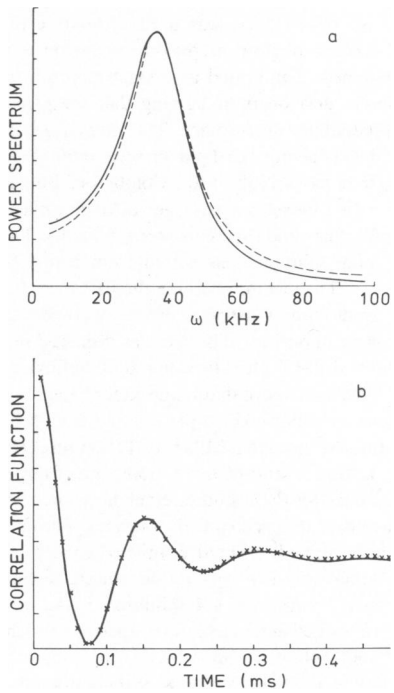

FIGURE 3 (*a*) Theoretical spectrum of light scattered by capillary waves of $q = 1{,}025$ cm^{-1}, assuming $\gamma_0 = 3.87$ dyn/cm and $\eta = 1$ cP ($\gamma' = 0$). The Lorentzian approximations (---) to this spectrum is shown for comparison. (*b*) The correlation function (xxx) corresponding to this spectrum, compared with the best-fit function of the form of Eq. 8.

close to Y_{crit} the spectral form is more complex. The exact form of the spectrum is influenced by the magnitude of the transverse shear viscosity γ', which lowers the peak frequency and increases the line width.

Experimentally, photon correlation spectroscopy has been used, so that the autocorrelation function (rather than the spectrum) of the scattered light is measured. These two equivalent representations are related mathematically by Fourier transformation (Fig. 3). In the propagating regime the correlation function can be approximated by

$$G_q(t) \simeq A + B \cos(\omega_0 t + \phi) \exp(-\Gamma t) \quad (8)$$

where the phase term ϕ is included to allow for the deviation of the spectrum from an exact Lorentzian form. In the nonpropagating regime the correlation function is, approximately,

$$G(t) \simeq \sum_{i=1,2} A_i \exp(-\Gamma_i t). \quad (9)$$

The variety of interfacial viscoelastic moduli has already been discussed. The transverse dilational modulus does not enter the theoretical treatment of capillary waves. For a symmetric membrane the in-plane dilational modulus (elastic compressibility) and the in-plane shear modulus do not affect the present experiments at all. Indeed, the only accessible modulus is that for the transverse shear (Eq. 1). These various independent moduli must be measured by specific techniques; the individual values found for a particular membrane need not be related.

MATERIALS AND METHODS

Membranes

General Considerations. Glycerol - 1.2 - monooleate (>99% purity, ~95% l-isomer, ~4% 2-isomer) in crystalline form (Sigma Chemical Co., St. Louis, MO) was used without further purification. Thin layer chromotography was used to check the purity of the lipid. For all samples examined, it migrated as a single spot on thin silica layers using two different developers, indicating that the glycerol monooleate (GMO) was predominantly l-isomer. The membrane-forming solution was made up by dissolving the lipid in several milliliters of *n*-decane (Puriss grade from Koch-Light Ltd., Colnbrook, England) which had been further purified by several passages through an activated alumina column to remove polar and surfactant contaminants. The concentration of the film-forming solutions was varied from 5 to 12 mg GMO per milliliter of decane. The medium bathing the BLM was 0.1 M NaCl. The NaCl (Ultrar grade) was roasted at 300°C overnight to drive off any volatile and organic impurities. The salt was dissolved in polished water, from a Millipore (Milli-Q) ultra-filtration unit Millipore Corp, Bedford, MA, with resistivity well above that required for "equilibrium water." All aqueous solutions were buffered to pH 6.0 and degassed. Before use all solutions were filtered through a Millipore Teflon filter (0.22 μm).

Membranes lasting several hours or more, and of large area (3–6 mm diam) were necessary for these studies. Such large membranes are rather susceptible to acoustic and mechanical vibrations. The disturbances could be minimized by using only a small volume of aqueous medium. Therefore the cell holding the BLM was a 1-cm square section glass spectroscopic cuvette containing only 3–4 milliliter of the aqueous medium. Membranes were formed across a circular aperture punched in a thinned section of a smooth Teflon septum which fitted diagonally into the cell. The Van den Berg method (12) was used as it is suited to the formation of large area BLM. The cell was sealed at the top and a 21 gauge hypodermic needle provided the only communication with the interior. A small quantity (5 μl) of the film forming solution was deposited upon the aqueous medium via this needle, which was also used to manipulate the septum for film formation. Prior to BLM formation the entire apparatus (particularly the septum) was scrupulously cleaned. This was the most important factor in ensuring long-lived membranes and reproducible results. Before BLM formation, the aqueous phase was pre-equilibrated with a minute quantity of the membrane-forming solution. Also, several hours were allowed to elapse after bilayer formation before taking measurements to ensure that the entire system had achieved thermodynamic equilibrium.

The cell was mounted with rotational and translational degrees of freedom to permit precise alignment of the membrane in the optical system. The entire cell assembly was placed upon a slab of expanded polystyrene to attenuate vibrations that appeared to arise from the circulation of cooling water in the laser. Acoustic disturbances were reduced by enclosing the cell and its mount in a perspex box having access apertures for the laser beams, etc. The entire apparatus (including optical system) was mounted on a massive steel table supported and leveled by pneumatic antivibration mounts.

Solvent-Free Membranes. It is known (13) that the proportion of solvent incorporated in membranes decreases as the chain length of the solvent molecules is increased. Squalene ($C_{30}H_{50}$), a long linear hydrocarbon, is essentially insoluble in membranes formed from GMO (14, 15). For the experiments described here squalane (or 2,6,10,15,19,23 – hexamethyltetracosane, $C_{30}H_{62}$) was used in preference to squalene as it is chemically more inert and is more saturated. It can be obtained in a purified form, avoiding the tedious purification processes and the difficulties of storage associated with squalene. Squalane was pure grade (98%) from Koch-Light. A very slight yellowish tinge indicated the presence of small quantities of impurities. These were removed by successive passages through 20 cm alumina columns until no discernible color remained. Because GMO is essentially insoluble in squalane, 10% (by volume) of *n*-hexane was added to the dispersion of GMO in squalane to dissolve any residual lipid crystallites. The *n*-hexane was allowed to evaporate just before forming the membrane. The thinning of these films was noticeably different from that of solvent-containing films; a very rapid transition to the black state followed upon the initial appearance of a black spot in the thinning film. The average lifetime of solvent-free membranes was much less than that of membranes formed from solutions of GMO in *n*-decane, but they did persist up to several hours. Due to this shorter lifetime some of the light-scattering experiments were initiated <1 h after membranes were formed. After such a short period the membranes were still adjusting to the boundary conditions at the aperture with considerable flexing, which caused some experimental difficulties; the low-tension membranes tended to change their plane of fixation.

Light Scattering

Design Considerations. Bimolecular lipid membranes have an extremely low reflectivity (typically $\sim 10^{-5}$), governed by the thickness (d) and refractive index (n_m) of the membrane. For the GMO/*n*-decane membranes used in the present work, values of $d = 55 \pm 5$ Å and $n_m = 1.43 \pm 0.01$ were measured using the method of Cherry and Chapman (16). Both are compatible with previous observations (17). The differential cross section for light scattering by capillary waves upon the membrane is (9)

$$\frac{1}{I_0}\frac{dI}{d\Omega} = \frac{k_B T}{\gamma_0 q^2}\frac{4\pi^2}{\lambda^4} n_m^2 r_{s,p}^2 \cos^3(\theta)$$

where $r_{s,p}$ are the Fresnel coefficients for aqueous/lipid interfaces at an angle of incidence θ. The scattered intensity is several orders of magnitude below that for the free surface of a liquid, due to the similarity of n_m and the refractive index of the surrounding fluid ($n = 1.33$) and the almost complete destructive interference of light reflected from the individual membrane interfaces. High incident light powers (~150 mW) were required to obtain satisfactory signals from BLM. To optimize the scattered-light intensity, laser light polarized perpendicular to the plane of incidence was used.

Visual observation showed that solvent-free membranes were noticeably blacker, reflecting the comparative absence of residual solvent. The refractive index of membranes formed from GMO in squalene is 1.45 ± 0.01 (18), higher than that for GMO/*n*-decane membranes. This enchances the scattering of light, leading to an improved signal-to-noise ratio in the observed correlation functions.

Experimental Arrangement. The light-scattering apparatus, basically a modified form of that used to study liquid surfaces (5), is sketched in Fig. 4. As it has been fully described elsewhere (19), only a brief description is required. The membrane was carefully oriented with its normal in the plane of incidence of the laser beam, which was directed upon the BLM at an angle θ. Capillary waves scattered light in a direction determined by

$$\mathbf{q} = \mathbf{k}_s - \mathbf{k}_0$$

where $\mathbf{k}_0$ and $\mathbf{k}_s$ are the wave vectors of the reflected and scattered light, respectively. The detector was placed far ($\geq$ 1 m) from the membrane to allow scattered light at low $\mathbf{q}$ to separate sufficiently from the reflected beam to permit definition of $\mathbf{q}$.

An argon ion laser (Lexel, model 85, Palo Alto, CA) was operated in the TEM_{00} mode at λ = 488 nm. The laser incorporated an intracavity etalon, and a light-regulator unit stabilized the intensity. No evidence could be found for low-frequency fluctuations ($\leq$ kHz) in the laser output power. The laser beam was spatially filtered to ensure a smooth Gaussian intensity profile.

To obtain a well-defined reflected beam, the incident beam should only illuminate a planar portion of the membrane; this restricts the beam diameter (D_0) at the membrane. However, unless $D_0 q >> 2\pi$, instrumental effects (see below) become very large. These conflicting requirements can be satisfied, provided the beam is focused somewhat beyond the membrane. In the present work, the beam (D_0 = 0.48 mm) was focused to a point 20 cm beyond the membrane with a convergence angle of 5.16 mrad. The low convergence angle permits light scattered at angles <1° to separate from the specular reflection.

To measure the frequency shift of the scattered light a reference beam was mixed with the scattered light at the photomultiplier. This beam was generated from the specularly reflected beam by a weak low dispersion diffraction grating placed close to the membrane. One of the diffraction orders was selected by an aperture in front of the detector, where it acts as reference beam for scattered light coincident with it. The grating constant

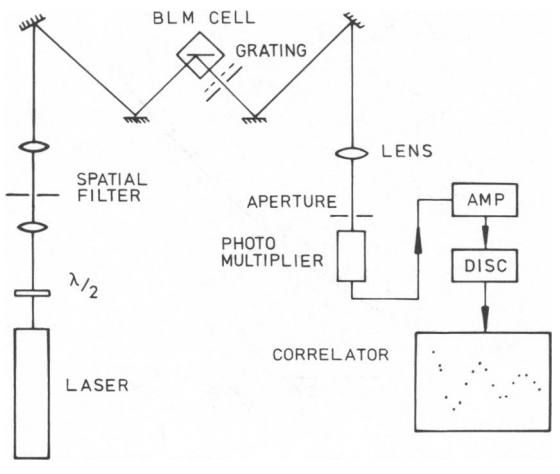

FIGURE 4 The experimental arrangement. A half-wave plate ($\lambda/2$) was used to set the plane of polarization on the laser beam accurately normal to the plane of incidence. The labeled lens is the cylindrical lens discussed in the text.

d defined the q value via

$$d = 2\pi n \cos\theta / q$$

where n is the order selected. The definition of q was more precise than if flare light were used as the reference beam and the reference beam intensity was controllable.

The cuvette holding the membrane had optically polished inner and outer surfaces to minimize stray or flare light. The cell was oriented to direct reflections at air-glass surfaces away from the photomultiplier. A diaphragm placed close to the grating was adjusted to suppress any stray light that did escape.

Provided the angle of scattering exceeds the convergence angle of the beam, the scattered light will separate from the reflected beam, so that the diffracted beams (and the scattered light) will be well defined in the detector plane. In practice, the peak of a reference spot is located precisely by scanning with a photodetector.

Despite the antivibration precautions taken, the laser beam reflected from the membrane oscillated somewhat at the photomultiplier. These oscillations tended to be normal to the plane of incidence. Their amplitude was reduced by a cylindrical lens of short focal length (Fig. 4), focusing the beam in a direction transverse to the plane of incidence and reducing the reference spots to linear filaments of Gaussian intensity profile. Use of this lens also led to an increase in the light flux at the detector.

The diaphragm in front of the detector was sized to avoid spatial averaging of the scattered light and to accommodate most of the residual excursions of the reference beam within the plane of incidence. In practice, a diameter of 0.5 mm was found suitable.

The photomultiplier output was processed by a fast amplifier discriminator designed for photon counting (20). Signal analysis used a 96-channel Malvern clipping correlator. The speed and efficiency of photon correlation is ideally suited to an analysis of the very low scattered intensities encountered with BLM.

Instrumental Effects. Correlation functions observed in this work have Γ values exceeding those expected. This instrumental effect arises from the finite angular acceptance of the detector within which capillary modes with differing frequencies are detected simultaneously. The observed spectrum is a convolution of the true spectrum with an instrumental function. In the time domain the process of convolution becomes multiplication; data fitting for photon correlation is considerably simpler.

The instrumental effect originates in the illumination of a limited number of oscillations of the capillary mode giving rise to a diffracted spot of finite extent in the image plane. The observed Gaussian intensity profile of the incident laser beam implies that this spot (and hence the instrumental function) has a Gaussian form. The correlation function corresponding to the convolution of a nearly Lorentzian spectrum (Eq. 7) and a Gaussian instrumental function (19) is

$$G(t) = A + B\cos(\omega t + \phi)\exp(-\Gamma t - \beta^2 t^2/4), \quad (10)$$

which accounts exactly for the excessive damping, and which can be fitted directly to the observed correlation functions. The factor $\beta^2/2$ represents the variance of the instrumental function in the frequency domain.

The relative effect of β decreases with increasing q, as β scales as $q^{1/2}$ whereas Γ scales as q^2. Experimentally it was found that for $q \geq 1{,}000$ cm^{-1}, essentially identical values of Γ were deduced whether Eq. 8 or 10 was used to fit the data.

It is possible to calculate β from considerations of the optical system. The β values deduced by fitting Eq. 10 to observed correlation functions somewhat exceed the calculated values, because we were unable to completely isolate the system from acoustic or mechanical disturbance of the membrane. Careful selection of the diaphragm in front of the detector to accommodate the excursions of the reference beam minimized the effect of such disturbances.

As noted by Grabowski and Cowen (1), a very broad instrumental

function will, together with the variation of scattered intensity with $1/q^2$, cause the peak frequency of the spectrum to shift to lower values. This effect was carefully evaluated. For instrumental line widths in the range found in the present work ($\Delta q \sim 50 - 120$ cm^{-1}) the frequency shifts are so low as to be negligible (19).

EXPERIMENTAL RESULTS

GMO/*n*-decane Membranes

For the initial set of experiments, membranes were formed from solutions containing 5 mg/ml GMO in *n*-decane. All experiments were carried out at room temperature (20 ± 1°C). Typical correlation functions are shown in Fig. 5. Frequencies (ω_0) and damping constants (Γ) were extracted by fitting the observed data to the functional form of Eq. 10 using a nonlinear minimization routine. Omission of the phase term ϕ led to significantly correlated residuals, confirming that the observed spectrum was not exactly Lorentzian. However, values of ϕ found in these fits were very susceptible to noise on the observed correlation functions. In some cases (at low q), clear separation of instrumental and true line widths (β and Γ) was not achieved, due to the limited duration of the time varying part of the data (Fig. 5).

The values of ω_0 and Γ derived at a given q can be interpreted in terms of the interface tension (γ_0) and the viscosity (η) of the ambient fluid, using the analytic approximations of Eq. 3. A set of data observed for one membrane is shown in Table I. Here the quantities ω_0 and Γ are obtained from a fitting procedure using Eq. 10, whereas the primed quantities illustrate the effect of neglecting the instrumental effects (i.e., using Eq. 8). The differences between ω_0 and ω_0' are small, and those between Γ and Γ' are largest at low q. All results quoted below derive from the values ω_0 and Γ.

The variability of data observed for different membranes formed from similar solutions represents the major source of uncertainty with the technique. This variability is illustrated in Fig. 6. Most notable is the greater spread in Γ than for ω_0. This simply reflects the inherently greater

TABLE I
DATA FOR MEMBRANE WITH 5 mg/ml GMO IN *n*-DECANE

Wave vector	ω_0'*	Γ'*	ω_0	Γ	γ_0	η
cm^{-1}	*krad/s*	s^{-1}	*krad/s*	s^{-1}	*dyn/cm*	*cP*
620	17.41	5.25	17.81	3.77	3.15	1.00
677	19.93	6.35	20.16	4.53	3.11	1.02
733	23.30	5.82	23.96	4.38	3.47	0.78
790	28.35	8.19	28.44	6.92	3.92	1.14
846	28.46	8.11	28.55	6.99	3.23	1.00
903	34.35	8.78	34.54	7.23	3.89	0.88
959	34.36	11.62	34.59	10.58	3.27	1.24
1,016	37.68	10.39	38.03	9.48	3.33	0.95
1,072	41.33	10.71	41.42	9.56	3.38	0.84
1,129	46.39	12.92	46.40	12.05	3.64	0.98

*In deriving ω_0' and Γ', the instrumental corrections were neglected.

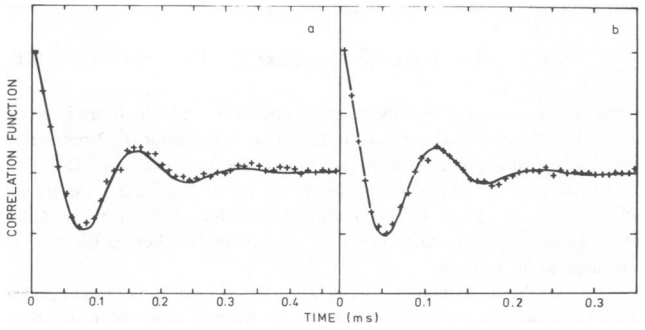

FIGURE 5 Correlation functions observed for GMO membranes at q of (*a*) 1,242 cm^{-1} and (*b*) 1,524 cm^{-1}. The different time scales should be noted. Only the time-varying portions of the function are shown. The lines are the best-fit functions of the form of Eq. 10. Typically such correlation functions require accumulation times of 1 min.

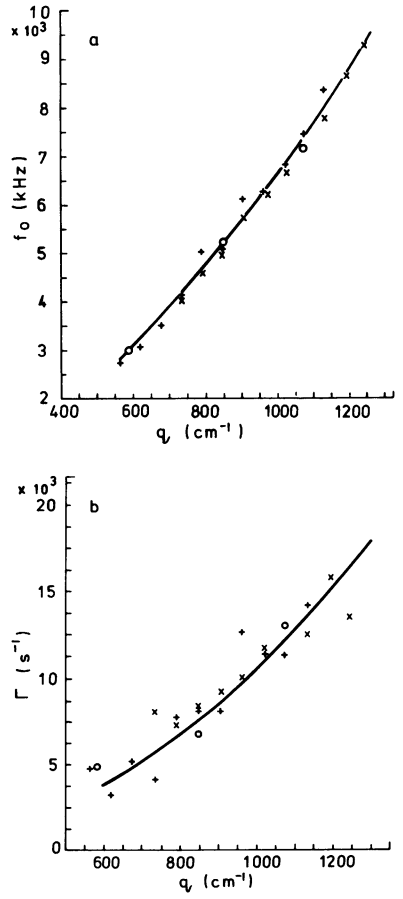

FIGURE 6 Variation of frequency (*a*) and damping constant (*b*) with q. The different symbols represent data taken on three separate occasions with membranes formed from solutions of the same composition. Shifting in the plane of fixation is evident from the form of the dispersion plot for one membrane (×).

precision in frequency measurements using photon correlation and the greater susceptibility of Γ to noise upon the correlation functions. Occasionally the plane of fixation of a membrane shifted slightly during an experiment, causing errors in the estimated wave vector. Such behavior is suggested by a discontinuous change in the dispersion curve (see Fig. 6). Average values of γ_0 and η for a given membrane were derived by fitting the dispersion plots to the analytic forms of Eq. 3. In this way data for all q were averaged.

Because of the variability discussed above, data for several membranes formed from similar solutions must be averaged. For membranes formed from solutions of 5 mg/ml GMO in *n*-decane, the mean tension was found to be 3.57 ± 0.25 dyn/cm. The viscosity of the surrounding medium was inferred to be 1.07 ± 0.30 cP. The agreement of this viscosity value with the accepted value (21) for 0.1 NaCl (1.025 cP at 20°C) suggests that the damping of the capillary waves in this case may be ascribed entirely to viscous dissipation in the aqueous medium. The tension is compatible with values previously found for membranes of GMO/*n*-decane. Haydon et al. (22) deduced a tension of 3.72 ± 0.20 dyn/cm for a film-forming solution of 8 mM lipid concentrations; White (personal communication) found γ_0 = 3.82 ± 0.03 dyn/cm for membranes formed from a solution of 3.6 mg/ml. Considering the higher lipid concentration in the present work and given the inherent small differences in the samples used, these values agree well with the present result.

The sensitivity of laser light scattering to modification of the interface tensions and the changes in the viscosity of the ambient fluid was investigated.

To study the sensitivity to small changes in BLM tension, membranes were formed from solutions containing varying concentrations of lipid. The tension of a black film is expected, from the Gibbs adsorption law, to depend only slightly on the lipid concentration in the film-forming solution. Membranes formed from a given solution do not precisely reflect the composition of that solution, but changes in the lipid concentration of the parent solution do apparently influence the composition of the final black membrane (13). The exact composition of the membrane depends upon the chain-length of the solvent used and the adsorption of the lipid molecules at the membrane interfaces.

For comparison with results obtained with the initial solutions membranes were formed from solutions containing 10 and 12 mg/ml. These membranes were more susceptible to mechanical disturbance, suggesting that their tensions were lower. For each solution used, several independent membranes were examined. This was necessary as membranes of low tension showed more tendency for the plane of fixation to vary. Averaging of the membrane properties is therefore particularly important. The values of Γ found showed almost no dependence upon the composition of the membranes (Fig. 7), indicative of the

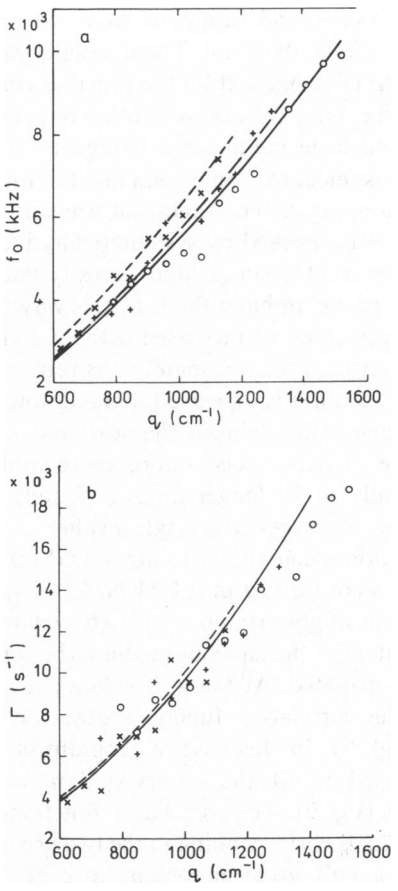

FIGURE 7 The frequencies (*a*) and damping constants (*b*) for membranes formed from solutions of different concentrations. Data for 5 (×), 10 (+), and 12 mg/ml (O) are shown, together with the dispersion curves (---, — —, ——) corresponding to the average tension and viscosity appropriate to each case. Note that the curves for Γ for the 10 and 12 mg/ml cases are not separable.

minor role played by tension in the imaginary part of the frequency (Eq. 3). The average viscosity values inferred for the aqueous medium were 1.09 ± 0.15 and 1.00 ± 0.12 cP for the 10 and 12 mg/ml cases, respectively. The frequency ω_0 at a particular q value decreased systematically with increasing lipid concentration (Fig. 7). The tensions

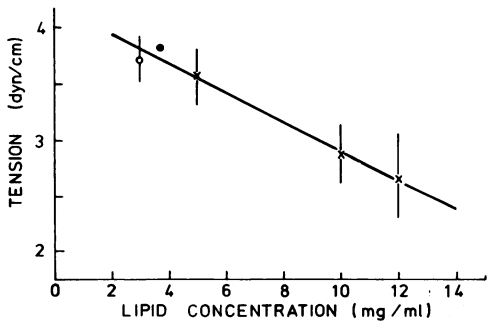

FIGURE 8 Variation of interfacial tension with lipid concentration of the film-forming solution. The data of Haydon et al. (O) (22) and White (●) (28) are also shown, together with the regression line for all the data.

deduced for the 10 and 12 mg/ml cases were 2.87 ± 0.26 and 2.67 ± 0.38 dyn/cm. These results continue the downward trend suggested by the previous comparison of tension for the 5 mg/ml case with other data (Fig. 8).

GMO/*n*-decane membranes bathed by 0.1 M NaCl appear to be subject to a single dominant damping mechanism, the damping of the evanescent wave in the aqueous phase. This was checked by systematically increasing the concentration of glycerin (a high viscosity liquid miscible with water) in the ambient fluid. In this way the viscosity of the medium could be increased without seriously altering its polarity (23). Unfortunately, the refractive index of the bathing medium is increased, tending towards that of the membrane. This reduced the scattered intensity. To improve the signal-to-noise ratio, correlation functions were accumulated for longer times (~5 min) and several functions were averaged at a single q value.

From solutions containing 10 mg/ml GMO in *n*-decane membranes were formed in 0.1 M NaCl solutions having concentrations of glycerin up to 40% (by volume). At 35% glycerin content in the aqueous medium the surface modes only just propagated. At lower Y values (i.e., larger q or larger η) the correlation functions observed were overdamped (Fig. 9). In this case, a program of Provencher (24) was used to fit the observed data to a sum of exponentials (Eq. 9). The correlation functions comprised two exponentials corresponding to the two predicted modes of Eq. 4. For 40% glycerin content, at q of 790 cm^{-1}, a single exponential mode was observed, indicating transition from oscillatory to overdamped fluid motion.

Where damped oscillatory correlation functions were observed, values of tension inferred (as previously described) were close to the value quoted above for the 10 mg/ml case: for 5 and 15% concentrations of glycerin, γ_0 was 3.09 ± 0.09 and 3.30 ± 0.53 dyn/cm, respectively. The apparent slight increase in γ_0 as η is increased may simply reflect the limited validity of the analytic approximations of Eq. 3 as Y approaches Y_{crit}. For overdamped correlation functions the two exponential decay constants suffice to determine both η and γ_0 (Eq. 4). For 40% glycerin concentration the tension found in this way was 2.99 ± 0.32 dyn/cm.

Viscosity values measured for the various glycerin concentrations are plotted in Fig. 10. The value for 40% (by volume) incorporates data for damped correlation functions with one or two exponential decay constants. The single exponential case yielded $\eta = 4.64 \pm 0.17$ cP, whereas the double exponential correlation functions gave 4.27 ± 0.44 cP, indicating the internal consistency of the method. The overall behavior of the data of Fig. 10 is in excellent agreement with the accepted variations of η with glycerin content (23). The slight deviations apparent in Fig. 10 at large glycerin content may well result from the inadequacy of the analytic approximations close to the transition region from propagating to nonpropagating modes. The damping of capillary waves on membranes due to the viscosity of the ambient medium can be measured reasonably precisely.

Membranes formed from solutions of GMO in *n*-decane incorporate a substantial fraction, estimated to be 37% (25), of solvent in their structure. In addition to the problem of disproportionation the retention of solvent introduces practical difficulties in the application of light-scattering methods. The solvent causes large deviations of the membrane from perfect planarity and may cause the local orientation of the film to vary over long periods. These changes in the orientation of the membrane surface relative to the incident laser beam lead to uncertainties in the wave vector of the capillary mode being studied. Solvent lenses in membranes make data acquisition very difficult. Whilst these lenses eventually disappear by coalescing with the Plateau-Gibbs border, leaving a more closely bimolecular membrane, this usually takes a long time. Some of these problems may be alleviated by the use of solvent-free BLM.

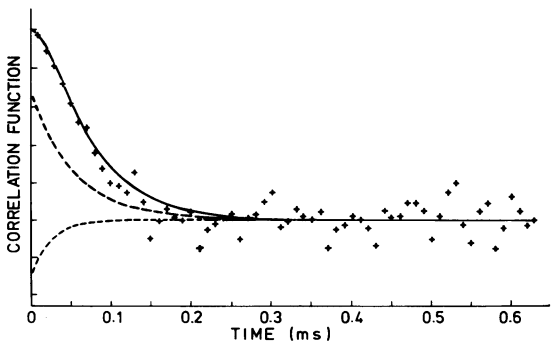

FIGURE 9 Over-damped correlation function observed at q = 1,020 cm^{-1} with 40% by volume glycerin added to the aqueous medium. The two exponentially decaying modes are shown separately (not normalized), as well as the total best-fit function (Eq. 9). The imperfect fitting around 150 μs may reflect the differences, close to Y_{crit}, of the spectrum from a sum of two Lorentzians centered on 0 Hz.

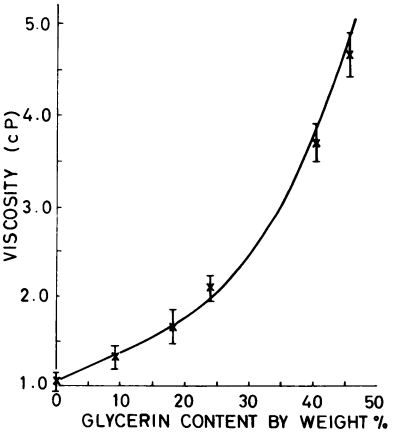

FIGURE 10 The measured viscosities of aqueous glycerin solutions. The experimentally used volumetric concentrations have been converted to percentages by weight for convenient comparison with the curve representing the accepted variation of η with glycerin content.

Solvent-Free Membranes

Membranes formed from GMO dispersions in squalene of three different concentrations (5, 10, and 15 mg/ml) were studied. The correlation functions observed had noticeably lower frequencies than those observed for BLM incorporating decane, indicative of the lower tension of the solvent-free membranes. Frequencies (ω_0) and damping constants (Γ) were derived by fitting the observed data with the appropriate functional form (Eq. 10).

Data for one membrane at each of the concentration used are shown in Fig. 11. The data for 15 mg/ml are obviously different in character from the rest and are discussed in detail below. The observed ω_0 and Γ values can be interpreted in terms of an interfacial tension (γ_0) and an apparent viscosity (η_{app}) for the ambient medium using Eq. 5, and assuming for the moment that $\gamma' = 0$ (see Table II). At $q \leq 790$ cm^{-1} the η_{app} inferred from Γ is greater than

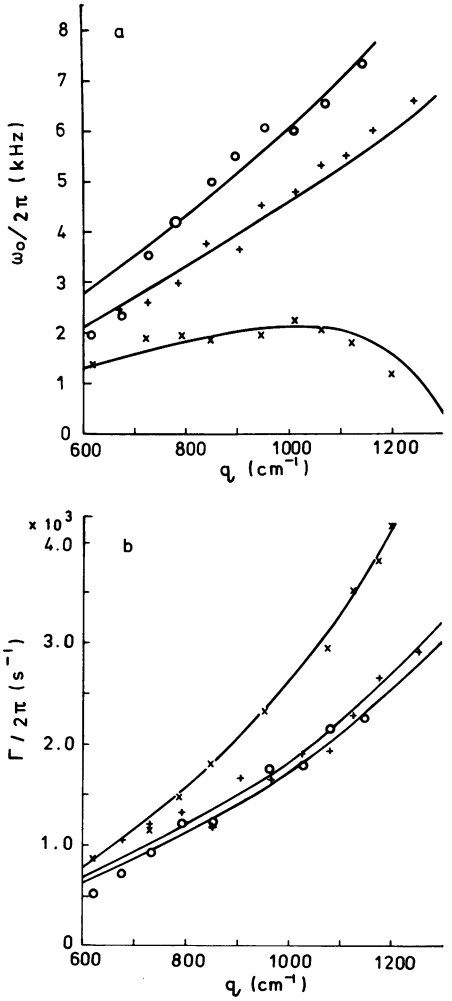

FIGURE 11 Variations of frequency (*a*) and line width (*b*) with q for membranes formed from solutions containing 5 (O), 10 (+), and 15 (×) mg GMO per ml squalane/hexane solution. The lines represent the dispersion plots calculated using the average values of γ_0 and γ' for each case, extracted from the fitted values of ω_0 and Γ (see text).

TABLE II
DATA FOR MEMBRANE WITH 10 mg/ml GMO IN SQUALANE

Wave vector	ω_0	Γ	γ_0*	η^*_{app}	γ_0‡	γ'‡
cm^{-1}	*krad/s*	*s^{-1}*	*dyn/cm*	*cP*	*dyn/cm*	*μsP*
677	15.44	7.60	1.76	1.84	2.25	47.5
734	16.39	7.72	1.56	1.59	1.97	30.9
790	18.22	8.42	1.42	1.50	1.94	24.2
847	23.37	7.39	2.07	1.10	2.40	4.1
903	22.81	10.60	1.63	1.44	2.04	19.0
959	28.15	10.24	2.07	1.21	2.45	8.2
1,016	30.41	12.07	2.03	1.29	2.45	10.6
1,072	33.62	12.07	2.10	1.15	2.50	5.0
1,120	34.31	14.43	1.93	1.14	2.36	9.3
1,169	37.48	17.08	2.02	1.14	2.53	12.8
1,253	38.37	18.34	1.72	1.16	2.19	9.5
1,300	39.77	20.11	1.66	1.15	2.14	10.1

The physical properties quoted were evaluated from ω_0 and Γ using Eq. 5 and various assumptions:
*Derived assuming $\gamma' = 0$ sP.
‡Derived under the assumption $\eta = 1.025$ cP.

that at higher q values, suggesting that β and Γ may not be fully separated at such low q values. No data at these low q values have been used in the following. This may be overly conservative, as in many cases (see Fig. 11) data for these q values are compatible with those at higher q. Note (Table II) that η_{app} exceeds the accepted value (1.025 cP) for 0.1 M NaCl. Fluctuations of γ_0 and η_{app} with q reflect the fluctuations in time of the orientation of a single membrane; variations are also observed arising from the inherent variability of membranes formed from identical solutions. These uncertainties were overcome by averaging the derived physical properties (γ_0 and either η_{app} or γ' as appropriate) over all q values observed (>790 cm^{-1}) and over all membranes studied of a particular type.

The data for BLM formed from the most concentrated dispersion (15 mg/ml) clearly differ in form from the rest of the data. At $q > 1{,}200$ cm^{-1}, ω_0 was essentially zero and Γ was very large, corresponding to the overdamped regime. Below this q value the capillary waves approached the critical region. While the expression for ω_0 in the propagat-

TABLE III
PHYSICAL PROPERTIES OF MEMBRANES FORMED FROM DISPERSIONS OF GMO IN SQUALANE

Lipid concentration	γ_0*	η^*_{app}	γ_0‡	γ'‡
mg/ml	*dyn/cm*	*cP*	*dyn/cm*	*μsP*
5	3.01 ± 0.85	1.21 ± 0.07	3.50 ± 0.98	8.3 (±3.7)
10	1.84 ± 0.21	1.20 ± 0.10	2.12 ± 0.25	7.8 (±4.6)
15	1.51 ± 0.14	1.74 ± 0.14	0.98 ± 0.14	3.8 (±1.4)

*Derived from ω_0 and Γ through Eq. 5, assuming $\gamma' = 0$ sP.
‡Found by substituting ω_0 and Γ in S_r and S_i in Eq. 2 and solving, with the assumption $\eta = 1.025$ cP.

ing regime (Eq. 5) can only be approximately correct, it was used to derive values of γ_0 and η_{app}.

Average values of γ_0 and η_{app} are shown in Table III for the three concentrations of film-forming dispersion used. The tension decreases with increasing lipid concentration, as was found for membranes formed from solutions of GMO in *n*-decane. However, the apparent viscosity increases rapidly with concentration.

The discrepancy between η_{app} and its accepted value contrasts sharply with the reliable measurement of the viscosity of the aqueous bathing solution for the case of solvent membranes. The most probable explanation of the difference is that an additional damping intrinsic to the membrane affects the capillary waves. This seems consistent with the increased effect of greater concentration of lipid in the film-forming solution.

If the viscosity of 0.1 M NaCl is assumed to be 1.025 cP, Eq. 5 can be used to deduce values of γ_0 and the transverse shear viscosity γ' of the interface from the fitted values of ω_0 and Γ. The last columns of Table II show such values for one membrane at different q values. The changes in γ_0 from the values found assuming $\gamma' = 0$ arise from the appearance of q (via τ') in the correction terms of Eq. 5.

Values of γ_0 and γ' obtained thus are limited in their accuracy by the assumption used in the derivation of Eq. 5 that $\tau' < 0.5$. In particular, the data for 15 mg/ml involves τ' values close to or above this limit. Clearly in such circumstances the approximate analytic formulae are inappropriate. Direct solution of the dispersion equation leads to more reliable estimates of γ_0 and γ'.

With the observed values of ω_0 and Γ, the real and imaginary parts of the dispersion equation (Eq. 2) provided two nonlinear simultaneous equations, which were solved for γ_0 and γ', assuming again $\eta = 1.025$ cP. This was done for all membranes (for $q > 790$ cm^{-1}) and the average values of γ_0 and γ' so derived are shown in Table III. The lines drawn through the observed data in Fig. 11 represent the frequencies and damping constants found by solutions of the dispersion equation using these average values of γ_0 and γ'.

At wave vectors above 1,200 cm^{-1}, the correlation function observed for the 15 mg/ml case displayed no discernible propagation, indicating overdamping (3). Such correlation functions were well-fitted by a sum of two exponentially decaying components (24) (Eq. 9). The Γ values of the two components yielded $\gamma_0 = 1.2$ dyn/cm and $\gamma' = 3.2 \times 10^{-5}$ sP (using Eq. 6 and with $\eta = 1.025$ cP). These values are in reasonable agreement with the data derived from propagating modes (Table III).

DISCUSSION

The results presented here show that the interfacial tension of GMO membranes can be measured reasonably accurately and reproducibly by photon correlation. The viscosity of the fluid surrounding the membrane is also measurable, suggesting that some difficulties previously encountered (1) have been overcome in the present work. The major source of uncertainty in the data remains the instrumental effect, particularly at low q. The instrumental functions were enlarged by the incomplete isolation of the system from low frequency vibration, by residual flare light, and by local curvature of the BLM (increasing the divergence of the laser beam). Inadequate correction of the instrumental effect can lead to increased values for the viscosity of the ambient solution. The instrumental effect decreases in significance as q increases, asymptotically disappearing.

Laser light of the high intensities necessary for these experiments could, particularly if focused, introduce problems due to absorption. The major effect would be the generation of thermal gradients and consequent convection currents. However, BLM are optically transparent ultrathin films ($<<\lambda$) so that the absorption of light will be minimal. The principal absorption bands of GMO and *n*-decane lie in the infrared, further reducing any problem due to this effect. Optical absorption is more likely to occur in the aqueous phase, due to the presence of minute quantities of impurities. The absence of convective motion in the system was experimentally verified (19).

The most serious limitation on the precision of the measurements relates to the membrane itself; its composition, planarity and stability being difficult to control. This variability is demonstrated by the fluctuating accuracy with which the properties of any individual membrane can be measured. Experimentally the most serious limitation results from the instability of the membrane. Data acquisition is severely complicated by the periodic shifting in direction of the normal to the membrane, occurring over periods of several minutes to one hour. Such changes lead to uncertainty in the angle of incidence of the laser beam upon the membrane. This motion certainly contributed to scatter in the data. However, several hours after the BLM formation the amplitude of this oscillation appears to decline. The use of *n*-decane as solvent for the lipid rather than shorter chain alkanes leads to BLM that are more stable and more nearly bimolecular on the average. However, the residual solvent within the membrane may disproportionate into small regions of bulk hydrocarbon (lenses). These scatter light intensely, adding uncontrollably to the reference beam. This, together with flare light from small particles in the bathing solutions and from the optical components may cause noisy correlation functions, particularly at small scattering angles. Noise can be partially suppressed by accumulating each data set over a longer time and by averaging several independent correlation functions taken at the same q value.

Correlation functions observed for individual membranes had widely differing signal-to-noise ratios, so that the physical properties were not always determined with the same accuracy. The overall precision in this work ranged from 5–15% for tension and 10–30% for viscosity.

The variation of measured tension with lipid composition of the film-forming solution demonstrates the sensitivity of the technique to rather small modifications of the properties of the system. The reduction in tension with increasing lipid concentration is consistent with an increase in the lipid packing density, probably at the expense of residual solvent in the BLM (26). The lipid concentration at the membrane interfaces is indeed influenced by the composition of the parent solution.

The apparent variation of γ_0 with concentration seems rather rapid. No data suitable for direct comparison over the concentration range covered appears to exist. The trend evident in Fig. 8 is comparable with the variation over the same range of concentration for bilayers of GMO/hexadecane (27). The variation for bulk GMO/*n*-decane in contact with 0.1 M NaCl at lower concentrations (13) does not overlap the present data (an extrapolation by a factor of 5 in concentration is required). The rather low precision of the present tension values does not permit definitive interpretation of the concentration dependence.

For the case of solvent membranes, the consistency of all viscosities measured for the bathing solution with accepted figures strongly suggests that the predominant damping of the capillary waves on these BLM arises from the evanescent wave in the aqueous phase.

In particular, changes induced in this damping by modification of the adjoining fluid can be reliably monitored. The results at zero glycerin content demonstrate that instrumental effects have been properly allowed for in the data analysis and the damping must be dominated by the aqueous phase. The results for high glycerin concentration cover a significant regime of the hydrodynamic theory, extending from $Y > Y_{crit}$ through the critical region to $Y < Y_{crit}$. Unfortunately in the latter area (high q values, glycerin content = 40%) the reliability of the correlation data decreases due to the falling signal-to-noise ratio. However, the viscosity values measured are close enough to the accepted values to suggest the approximate validity of the theory in the region $Y \sim Y_{crit}$.

Investigation of solvent-free membranes is important as they are more closely bimolecular than those containing solvent. Whereas BLM incorporating decane are clearly fairly fluid structures, membranes lacking solvent display a much reduced fluidity (i.e., an observable viscosity). Thus the presence of solvent in a bilayer influences the properties observed for the membrane. This fact emphasizes that care should be taken in extrapolating from observations on model membranes to biomembranes.

The tension values for membranes formed from dispersions of GMO in squalane are lower than for GMO/*n*-decane membranes, thus attesting to the comparative absence of solvent in these membranes. The tension decreases further with increasing lipid concentration in the film-forming solution. White (28) has studied the variation of solvent content of BLM formed from solutions of GMO in various solvents (at a lipid concentration of 20 mg/ml). Increase of the chain length of the hydrocarbon solvent decreased the solvent content of the final BLM and reduced the interfacial tension from 2.17 ± 0.23 dyn/cm for *n*-dodecane to 1.31 ± 0.19 dyn/cm for *n*-hexadecane. These values are compatible with those found in the present work despite the rather lower lipid concentrations in the parent dispersions.

Elliott and Haydon (29) report an interfacial tension of 1.0 ± 0.3 dyn/cm for solvent-free membranes formed from 28 mM GMO in squalane. The tension found here for the 15 mg/ml case (0.98 ± 0.14 dyn/cm) is thus consistent with the presence of little or no solvent in the bilayer. At lower concentrations the tension values may be influenced by the retention of some hexane in the BLM. In this complex system interpretation of the apparent decrease in γ_0 with lipid concentration is not straightforward.

Although the large apparent viscosity inferred for the aqueous medium adjoining the membranes could be explained by a large error in the detected q values, the magnitude of error involved would be quite outside the uncertainties involved in the present work. The excessive values of η_{app} for solvent-free BLM were observed for all q values, suggesting the reality of the effect and the necessity of its interpretation in terms of an intrinsic membrane viscosity. The appearance of the transverse shear viscosity γ' of solvent-free membranes is compatible with an increase in the lipid packing density.

The enhanced damping due to internal membrane effects causes the transition from oscillatory to overdamped motion to occur at Y greater than the critical value found for a membrane with $\gamma' = 0$ (see above). This transition is observed at a relatively low q value for the highest lipid concentration used here, supporting the above interpretation in terms of an intrinsic membrane viscosity. The values of transverse shear viscosity observed for this case are compatible with the value $\gamma' = 3.5\ (\pm 1.4) \times 10^{-5}$ sP (surface poise) observed for fully condensed monolayers of GMO on an aqueous substrate (30).

This intrinsic membrane viscosity may result from an increased interaction between the hydrocarbon chains of the lipid molecules which would be somewhat reduced in the presence of a solvent medium within the BLM interior. Whereas short-chain solvents such as decane can be accommodated close to the center of the membrane, the above results indicate that long-chain solvents are, for the most part, excluded from the bilayer region. This exclusion arises as such solvents have no polar groups to prevent energetically unfavorable water-hydrocarbon contacts at the bilayer interfaces, and as their internal degrees of freedom are restricted in the relatively ordered interior of the bilayer. While some uncertainty attaches to just how fully squalane is excluded from lipid bilayers (26), the present work together with that of White (14) suggests that membranes formed of GMO dispersed in squalane do contain substantially less solvent than those formed from solutions of GMO in decane. Visual observations of the

thinning of these membranes, in particular the rapid final transition to the black state, provides some additional, albeit qualitative, evidence of the strong molecular cohesion inferred from membrane viscosity and tension values.

The sensitivity of light scattering to γ' depends upon the magnitude of γ_0 (Fig. 1). The lower limit of γ' experimentally accessible for any particular system can only be established by careful consideration of the dispersion equation (cf. Fig. 2) for the appropriate tension. For membranes with $\gamma_0 \leq 3$ dyn/cm, it appears that $\gamma' \sim 10^{-5}$ sP would be about the lowest measurable value. More reliable estimates of very low γ' could be obtained from data at large q; however, presently experiments are limited to $q <$ 2,000 cm^{-1}.

In the only previous experiment in this area, Grabowski and Cowen (1) investigated BLM of oxidized cholesterol, using light scattering and encountered some of the difficulties already mentioned. Their data interpretation was based upon a specific model considering the membrane as a single interface between two fluids. The properties so deduced must refer to the membrane as a whole, rather than to the individual lipid-water interfaces. They observed line widths some 50% greater than expected from the viscosity of the medium surrounding the membrane. To explain this they invoked an instrumental line width of 500 cm^{-1}, sufficient to cause an appreciable reduction of the peak frequency of the spectrum of the scattered light. After correcting for this effect they deduced a membrane tension of 2.5 ± 0.5 dyn/cm, rather above the accepted value of 1.9 dyn/cm for BLM of oxidized cholesterol. All capillary waves on these membranes were overdamped by the addition of 28% (by volume) glycerin to the ambient solution. For a tension of 2.5 dyn/cm, $Y_{crit} = 0.155$ implies that overdamping can only occur with a viscosity corresponding to a 34% solution of glycerin. This concentration causes overdamping ($Y < Y_{crit}$) for q = 1,500 cm^{-1}; higher concentrations are required for lower q values. This discrepancy between Grabowski and Cowen's observation and theoretical prediction may be resolved if the actual tension of the membranes was lower than the value quoted. An independent argument for such a lower tension derives from the wave frequencies. If the frequencies observed by Grabowski and Cowen are accepted as representing ω_0, Eq. 3 suggests that the tension of their membranes was ~1.8 dyn/cm, close to the accepted value. The excess line widths can be understood if the capillary waves are damped by dissipative processes associated with the oxidized cholesterol membrane. It is interesting to note that the addition of pure cholesterol to GMO/decane membranes causes just such additional damping (31).

CONCLUSION

The results of this paper confirm that the mechanical properties of monoglyceride BLM can be measured reliably by photon correlation spectroscopy. The method is essentially nonperturbative and is unique among spectroscopic techniques for membranes in that adequate signal strength is obtained from a single black film. The technique seems likely to be most useful in monitoring changes in, rather than the absolute values of, the viscoelastic parameters of membranes.

Laser-light scattering provides a novel method for investigating the fluidity of membranes. The shear interfacial viscosity which acts normal to the membrane plane (the dynamic component of interfacial tension γ'), is not measureable using molecular probe techniques such as fluorescence correlation spectroscopy or fluorescence photobleaching recovery so that photon correlation provides information complementary to that obtained by these methods. In particular, the viscosity γ' is a macroscopic quantity referring to the entire membrane structure, whereas viscosities inferred from diffusion-based methods may result from only localized molecular interactions within the membrane (32).

Theoretically, in the case of asymmetric membranes, the compression and transverse fluctuations become coupled. Other viscoelastic properties of the membrane would enter the hydrodynamic description of fluid flow associated with these fluctuations. It is, however, difficult to envisage experimental situations that could take advantage of this coupling, as the necessary large differences between the fluids would probably jeopardize the stability of the membrane. However, the elastic compressibility and its associated interfacial viscosity (dilational within the membrane plane) directly affect the propagation of compression waves on the membrane. For Y far below Y_{crit} it is expected theoretically that such compression modes become important. While these modes scatter light much less strongly than transverse waves (9) it is possible that sensitive experiments in this regime would permit measurement of these membrane properties.

APPENDIX

Analytic approximations to the roots of Eq. 2 are required for the regimes $Y > Y_{crit}$ and $Y < Y_{crit}$. Eq. 2 can be manipulated into the form

$$2S^4 + S^3 + 4YS^2 + 2YS + 2Y^2 = 0. \quad \text{(A1)}$$

This may be factorized into two quadratic terms, subject to the constraint that any remainder terms should vanish. Then

$$(S^2 + aS + b)\,[2S^2 + (1 - 2a)\,S + 2(2Y - b) - a(1 - 2a)] = 0. \quad \text{(A2)}$$

Thus, either of the quadratic factors may be zero, subject to the conditions

$$2Y^2 - b[2(2Y - b) - a(1 - 2a)] = 0 \quad \text{(A3)}$$

and

$$2Y - b(1 - 2a) - a[2(2Y - b) - a(1 - 2a)] = 0. \quad \text{(A4)}$$

A3 and A4 impose a unique functional dependence of a and b upon Y. These equations were solved numerically over the physically interesting

range of Y(0–10). The results indicated that a and b were well-behaved functions of Y, having different dependence upon Y in the regime $Y > 1.0$ and for $Y < 1.0$. Apart from a in the region $Y < 1.0$, linear approximations were adequate. The resulting approximate expressions for a and b are

$$Y > 1.0 \qquad a \simeq 0.85 + 0.03Y \qquad \text{(A5)}$$

$$b \simeq 0.05 + 0.83Y \qquad \text{(A6)}$$

$$Y < 1.0 \qquad a \simeq 0.5 + 0.25Y^{1/2} \qquad \text{(A7)}$$

$$b \simeq 0.53Y \qquad \text{(A8)}$$

where the coefficients are accurate to within 10%.

Inspection of the two quadratics in A2 shows that as a is strictly positive and >0.5, the physically realistic roots of Eq. A1 are given by the roots of

$$S^2 + aS + b = 0.$$

Using Eqs. A5 and A6 (i.e., low damping, $Y >> Y_{crit}$), the roots of A1 are thus

$$S = -\tfrac{1}{2}(0.85 + 0.03Y) \pm \tfrac{1}{2}i(3.4Y - 0.5225),$$

which gives Eq. 3, explicitly. The transition from oscillatory to overdamped behavior is set by $a^2 - 4b = 0$ which (with Eqs. A5 and A6) yields $Y_{crit} = 0.156$, close to the value found by numerical solution of Eq. 2.

In the regime $Y < Y_{crit}$, Eqs. A7 and A8 are used to solve for S. The resulting roots are

$$S_1 = -(0.5 + 0.25\sqrt{Y})$$

and

$$S_2 = -\frac{0.53\,Y}{(0.5 + 0.25\sqrt{Y})}$$

corresponding to Eq. 4.

This work was supported by a grant from the United Kingdom Science and Engineering Research Council. Dr. Crilly wishes to acknowledge financial support given by the Department of Education for Northern Ireland, and also useful discussions with Professor D. A. Haydon. Miss G. Crawford provided a computer program used to solve the dispersion equation.

Received for publication 5 April 1982 and in revised form 6 September 1982.

REFERENCES

1. Grabowski, E. F., and J. A. Cowen. 1977. Thermal excitations of a bilipid membrane. *Biophys. J.* 18:23–28.
2. Crilly, J. F., and J. C. Earnshaw. 1980. Photon correlation spectroscopy of lipid membranes. *In* Laser Advances and Applications. B. Wherrett, editor. John Wiley & Sons, Ltd., Chichester, England. 181–184.
3. Crilly, J. F., and J. C. Earnshaw. 1980. Photon correlation studies of model membranes. *In* Fourth International Conference on Photon Correlation Techniques in Fluid Mechanics. W. T. Mayo, Jr. and A. E. Smart, editors. Stanford University, Stanford, CA. 21.1–21.7.
4. Goodrich, F. C. 1981. The theory of capillary excess viscosities. *Proc. R. Soc. Lond. A.* 374:341–370.
5. Byrne, D., and J. C. Earnshaw. 1979. Photon correlation spectroscopy of liquid interfaces. I. Liquid-air interfaces. *J. Phys. D. Appl. Phys.* 12:1133–1144.
6. Hård, S., and R. D. Neuman. 1981. Laser light-scattering measurements of viscoelastic monomolecular films. *J. Colloid Interface Sci.* 83:315–334.
7. Evans, E., and S. Simon. 1975. Mechanics of bilayer membranes. *J. Colloid Interface Sci.* 51:266–271.
8. Kramer, L. 1979. Theory of light scattering from fluctuations of membranes and monolayers. *J. Chem. Phys.* 55:2097–2105.
9. Bouchiat, M. A., and D. Langevin. 1978. Relation between molecular properties and the intensity scattered by a liquid interface. *J. Colloid Interface Sci.* 63:193–211.
10. Goodrich, F. C. 1961. The mathematical theory of capillary. II. *Proc. Roy. Soc. Lond. A.* 260:490–502.
11. Brochard, F., and J. F. Lennon. 1975. Frequency spectrum of the flicker phenomenon in erythrocytes. *J. de Physique (Paris).* 36:1035–1047.
12. Van den Berg, J. H. 1965. A new technique for obtaining thin lipid films separating two aqueous media. *J. Mol. Biol.* 12:290–291.
13. Andrews, D., E. Manev, and D. A. Haydon. 1970. Composition and energy relationships for some thin lipid films, and chain configuration in monolayers at liquid-liquid interfaces. *Special Discussions Faraday Soc.* 1:46–56.
14. White, S. H. 1978. Formation of "solvent-free" black lipid bilayer membranes from glycerol monooleate dispersed in squalene. *Biophys. J.* 23:337–347.
15. Simon, S. A., L. J. Lis, R. C. MacDonald, and J. W. Kauffman. 1977. The noneffect of a large linear hydrocarbon, squalene, on the phosphatidylcholine packing structure. *Biophys. J.* 19:83–90.
16. Cherry, R. J., and D. Chapman. 1969. Optical properties of black lecithin films. *J. Mol. Biol.* 40:19–32.
17. Pagano, R. E., R. J. Cherry, and D. Chapman. 1973. Phase transitions and heterogeneity in lipid bilayers. *Science (Wash., D. C.).* 181:557–558.
18. Bach, D., and I. R. Miller. 1980. Glycerol monooleate black lipid membranes obtained from squalene solutions. *Biophys. J.* 29:183–187.
19. Crilly, J. F. 1981. Photon correlation spectroscopy of planar bilayer lipid membranes. Ph.D. Dissertation. Queen's University of Belfast.
20. Güttinger, H., M. Gautschi, and E. Serrallach. 1976. A low cost preamplifier/discriminator for fast photon counting. *J. Phys. E. Sci. Instrum.* 9:936–937.
21. International Critical Tables. 1928. National Research Council, New York. 5:12–19.
22. Haydon, D. A., and J. L. Taylor. 1968. Contact angles for thin lipid films and the determination of the London – van der Waals forces. *Nature (Lond.).* 217:739–740.
23. Sheely, M. L. 1932. Glycerol viscosity tables. *Ind. Eng. Chem.* 24:1060–1064.
24. Provencher, S. W. 1976. An eigenfunction expansion method for the analysis of exponential decay curves. *J. Chem. Phys.* 64:2772–2777.
25. Pagano, R. E., J. M. Ruysschaert, and I. R. Miller. 1972. The molecular composition of some lipid bilayer membranes in aqueous solution. *J. Membr. Biol.* 10:11–30.
26. Waldbillig, R., and G. Szabo. 1978. Solvent-depleted bilayer membranes from concentrated lipid solutions. *Nature (Lond.).* 272:839–840.
27. Benz, R., O. Fröhlich, P. Läuger, and M. Montal. 1975. Electrical capacity of black lipid films and of lipid bilayers made from monolayers. *Biochim. Biophys. Acta.* 394:323–334.
28. White, S. H. 1975. Phase transitions in planar bilayer membranes. *Biophys. J.* 15:95–117.

29. Elliott, J. R., and D. A. Haydon. 1979. The interaction of *n*-octanol with black lipid bilayer membranes. *Biochim. Biophys. Acta.* 557:259–263.
30. Crilly, J. F., and J. C. Earnshaw. 1982. The surface viscosity of fully condensed monolayers of glycerol monooleate. *In* Biomedical Applications of Laser-Light Scattering. D. B. Sattelle, W. I. Lee, and B. R. Ware, editors. Elsevier/North Holland, Amsterdam. 123–135.
31. Waldbillig, R. C., and G. Szabo. 1979. Planar bilayer membranes from pure lipids. *Biochim. Biophys. Acta.* 557:295–305.
32. Edidin, M. 1974. Rotational and translational diffusion in membranes. *Annl. Rev. Biophys. Bioeng.* 3:179–201.